

Analysis of high Reynolds numbers effects on a wind turbine airfoil using 2D wind tunnel test data

This content has been downloaded from IOPscience. Please scroll down to see the full text.

2016 J. Phys.: Conf. Ser. 753 022047

(<http://iopscience.iop.org/1742-6596/753/2/022047>)

View [the table of contents for this issue](#), or go to the [journal homepage](#) for more

Download details:

IP Address: 184.174.98.70

This content was downloaded on 20/01/2017 at 23:51

Please note that [terms and conditions apply](#).

You may also be interested in:

[Study of Reynolds number effect on turbulent boundary layer near the separation](#)

A Dród and W Elsner

[THE SIGNATURE OF INITIAL CONDITIONS ON MAGNETOHYDRODYNAMIC TURBULENCE](#)

V. Dallas and A. Alexakis

[A new criterion for end-conduction effects in hot-wire anemometry](#)

Marcus Hultmark, Anand Ashok and Alexander J Smits

[DNS experiments on the settling of heavy particles in homogeneous turbulence: two-way coupling and Reynolds number effects](#)

Anne Dejoan

[Isoenstrophy points and surfaces in turbulent flow and mixing](#)

Carl H Gibson

[Numerical study of similarity in prototype and model pumped turbines](#)

Z J Li, Z W Wang and H L Bi

[Flow and roller array interaction at low Reynolds numbers](#)

Zubair M Sheikh, Lipo Wang and Qiang Zhang

[A new formulation for the streamwise turbulence intensity distribution](#)

P Henrik Alfredsson, Ramis Örlü and Antonio Segalini

[Wind Tunnel Tests of Wind Turbine Airfoils at High Reynolds Numbers](#)

E Llorente, A Gorostidi, M Jacobs et al.

Analysis of high Reynolds numbers effects on a wind turbine airfoil using 2D wind tunnel test data

O Pires¹, X Munduate¹, O Ceyhan², M Jacobs³, H Snel²

¹ CENER (National Renewable Energy Centre), Avenida Ciudad de la Innovación 7, 31621 Sarriena, Navarra, Spain

² Energy research Center of the Netherlands (ECN), 1755LE, Petten, The Netherlands

³ DNW, Bunsenstrasse 10, 37073 Göttingen, Germany

E-mail: oepires@cener.com

Abstract. The aerodynamic behaviour of a wind turbine airfoil has been measured in a dedicated 2D wind tunnel test at the DNW High Pressure Wind Tunnel in Göttingen (HDG), Germany. The tests have been performed on the DU00W212 airfoil at different Reynolds numbers: 3, 6, 9, 12 and 15 million, and at low Mach numbers (below 0.1). Both clean and tripped conditions of the airfoil have been measured. An analysis of the impact of a wide Reynolds number variation over the aerodynamic characteristics of this airfoil has been performed.

1. Introduction

One of the aerodynamic issues that the design of the future generation of multi-MW turbines has to deal with is the increasing Reynolds numbers (above 10 million) that the new larger blades will be facing. The lack of experimental data on wind turbine dedicated airfoils above Reynolds 4 million, and thus, the few chances for codes validation at these conditions imply a high uncertainty on blade design and existing design tools.

Within EU FP7 AVATAR project (AdVanced Aerodynamic Tools of lArge Rotors) [1], a high Reynolds number and low Mach number wind tunnel test has been performed with the aim to obtain reliable data that can be used to validate existing aerodynamic models for this operating range. The test has been performed at the DNW High Pressure Wind Tunnel in Göttingen (HDG). This wind tunnel has a unique feature of increasing Reynolds number without changing the fluid and without increasing the Mach number of the flow. This gives opportunity to isolate the Reynolds number effects from other combined effects that might come from the compressibility or different fluid viscosity.

The tests have been performed over the DU00-W-212, a 21% thick wind turbine dedicated airfoil developed by Delft Technical University. This airfoil has been selected because of its transition behavior in pressure and suction side, as it helps to validate and improve the existing transition prediction aerodynamic models.

This paper presents an analysis of the measured aerodynamic coefficients and their variations with high Reynolds numbers.



2. Experiment description

2.1. Wind tunnel facility.

The wind tunnel test has been performed at the HDG wind tunnel, which is a closed return circuit with a closed test section of 0.6 x 0.6 m. (width x height) and 1 m. length, and a contraction ratio of 5.85. This tunnel can be pressurized up to 100 bars to achieve high Reynolds numbers. The wind tunnel speed is controlled by rpm regulation of the constant pitch fan in the range from 3.5 to 35 m/s, which allows for Reynolds number effect simulations with negligible Mach influence as it stays always below 0.1.

The cooling of the air flow, which is necessary at the higher Reynolds numbers, is done by a water film cooling system installed on the outer shell of the tunnel.

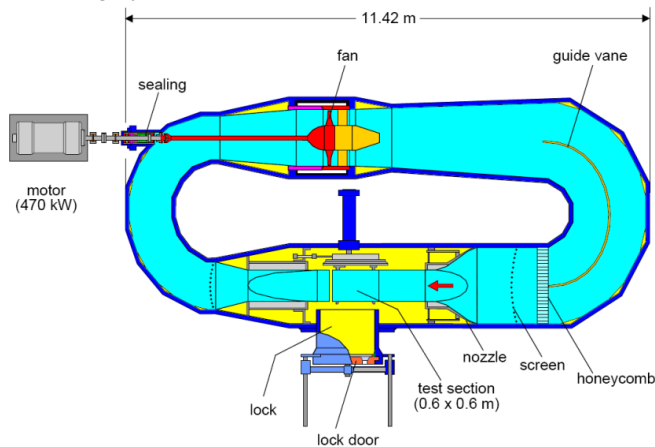


Figure 1. DNW HDG wind tunnel lay out

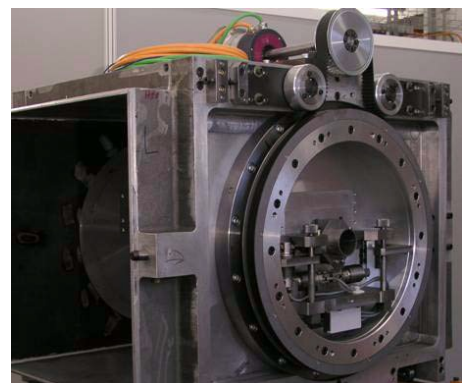


Figure 2. Test section lateral view showing alpha mechanism

The test section used for the measurements is a dedicated 2D test section where the model is horizontally installed in the mid part into a remote controlled alpha mechanism capable of performing 360° of angular setting of the model. Top and bottom wall centerlines are equipped with 23 pressure taps each, equally distributed over the whole length of the test section, that can be used to calculate wall interference properties (Method used is described in [2]).

2.2. Wind tunnel model.

A 150 mm. chord 2D model reproducing the shape of the TU-Delft DU00-W-212 airfoil was manufactured out of steel. The trailing edge thickness was increased to a 0.333% of the chord in order to allow for pressure tap installation in the trailing edge.

The model was equipped with 90 pressure taps with a diameter of 0.2 mm at the mid span. To avoid pressure readings being influenced by the taps, taps were aligned with a minimum angle to the chord of 10 degrees. Minimum distance of the center of the pressure taps was designed to be 2 mm, to allow for tube connection inside the model. Pressure taps were distributed to catch the predicted main flow features at operating conditions of the designed airfoil.

The model is installed in the test section center and rotates around the point at 1/3 of the chord from the leading edge.

2.2.1. Fixed transition implementation on the model. Transition tripping was performed by application of transition dots in the upper and lower surface of the model, at 5% and 10% respectively. All dots have the same diameter of 1.27 mm and a distance center to center of 2.54 mm.

Two different height combinations of dots have been used in the test: Trip1 and Trip2 (described in table 1). The Trip 1 showed to have very low effect compared to the clean configuration for the lower

Reynolds number cases. So, Trip 2 configuration was tested to assure the transition at the same locations for all the Reynolds numbers.

| Trip conditions: | | | |
|------------------|-------------------------------|-----|-------------------------|
| | Chord position (from L.E.) | | Dots height (mm.) |
| Trip 1 | Upper | 5% | 0.038 |
| | Lower | 10% | 0.079 |
| Trip 2 | Upper | 5% | 0.079 |
| | Lower | 10% | 0.102 |

Table 1. Description of transition tripping



Figure 3. View of dots installed in suction side (left) and pressure side (right)

Data shown in this paper correspond to the Trip 2 tripping conditions. Later publications will show the effects of the different tripping transitions.

2.3. Instrumentation.

Besides the pressure taps on the model, a wake rake with 118 total and 8 static pressure probes was installed around 2 chords downstream of the trailing edge of the model. Using a traversal mechanism it can be moved from centerline to the vicinity of one sidewall. As the model pressure taps of the model are at the mid span, the wake rake useful range to determine undisturbed drag is limited from 100 to 200 mm out of the centerline ($y = -100$ to -200 mm in test section coordinate system). The wake rake covers 300 mm in height around the center, allowing for the evaluation of the wake even at high angles of attack

Lift and Pitching Moment Coefficients were calculated by integration of the pressure distribution over the airfoil. Drag was calculated from the flow loss of momentum by integrating the total and static pressures in the airfoil wake.

Additional instrumentation has also been used, e.g.: a 3-component balance for correlation of the aerodynamic coefficients, 5 fast response Kulite sensors installed in the model for unsteady pressure measurements, a cylindrical hot-film probe for inflow speed fluctuation measurements and UV LED light and camera for oil flow visualization.

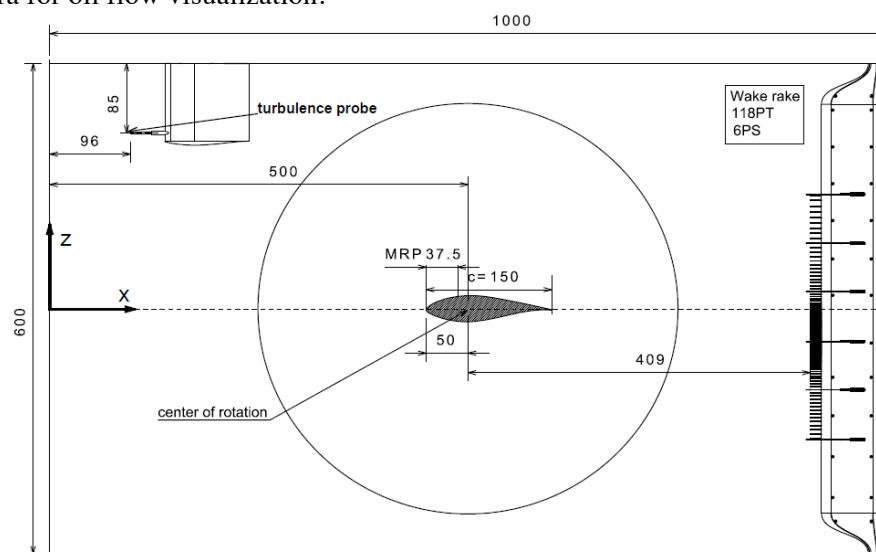


Figure 4. Test section sketch with model and instrumentation

2.4. Testing procedure.

The tests have been performed at 5 different Reynolds numbers: 3, 6, 9, 12 & 15 million, and at Mach numbers always below 0.1. For some Reynolds numbers tests have been performed at different Mach numbers, i.e. using different tunnel total pressure. For all the testing conditions the turbulence intensity level of the flow is always below 0.5%.

Each polar started at 0° angle of attack to do the positive angles sweep up to the maximum positive angle of attack, then the 0° was repeated to start the negative angles sweep to the maximum negative angle of attack. After that, some angles of attack were measured again to check repeatability. Classical corrections following the formulas of Allen and Vincenty [3], as well as corrections obtained from wall pressure distribution [2] were calculated for each data point. All the data shown in the paper have the corrections applied.

3. Results

The presented results are the aerodynamic coefficients obtained by integration of the pressure distribution over the airfoil (Lift Coefficient) and the integration of the total pressure distribution on the wake rake (Drag Coefficient), for both clean and tripped conditions

3.1. Data for the DU00-W-212 airfoil at clean conditions

Figure 5 shows the general trends of the aerodynamic coefficients for all the measured Reynolds numbers at clean conditions. The right plot shows the lift coefficient (C_l) against angle of attack (AoA) while the left plot presents the C_l against the drag coefficient (C_d) expressed in drag counts (D.C.).

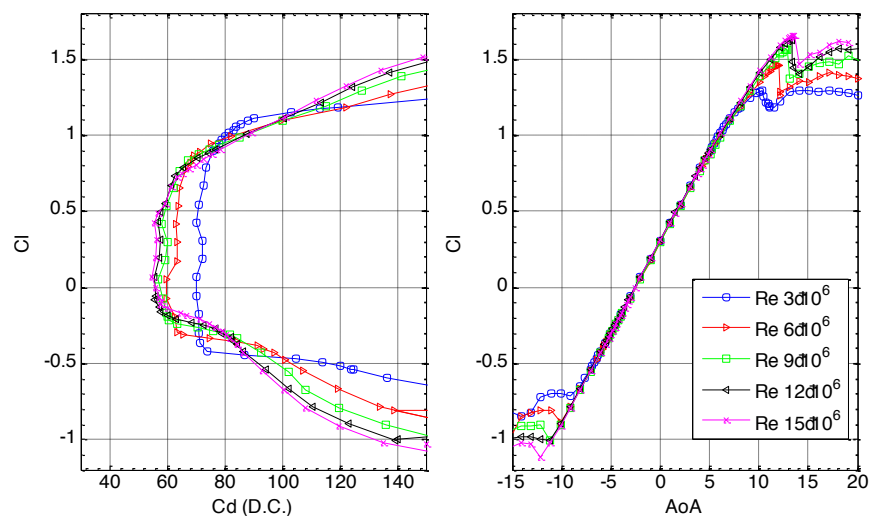


Figure 5. Clean condition aerodynamic coefficients. Lift vs Drag and Lift vs angle of attack

From the plots at clean conditions it is clearly seen, as expected [4] [5] [6] & [7], how the minimum drag decreases and the maximum lift increases with increasing Reynolds numbers. Also the laminar drag bucket gets narrowed as the Reynolds number increases, since transition position moves towards the leading edge (as it can be seen on the pressure distributions shown in figure 6).

Figure 6 shows the airfoil pressure distributions measured by the pressure taps and expressed in non-dimensional pressure coefficients (C_p) for an angle of attack of 2° and three different Reynolds numbers (3, 6 and 9 million). The three curves match quite well as it is expected for an angle of attack within the lift linear region. There are only some small areas, which are zoomed out in the figure, where there are significant variations. These areas correspond to the slope change of the pressure

distribution caused by the laminar to turbulent transition, in both the suction and the pressure side of the airfoil. For both cases we can see how the transition is earlier at the highest Reynolds number.

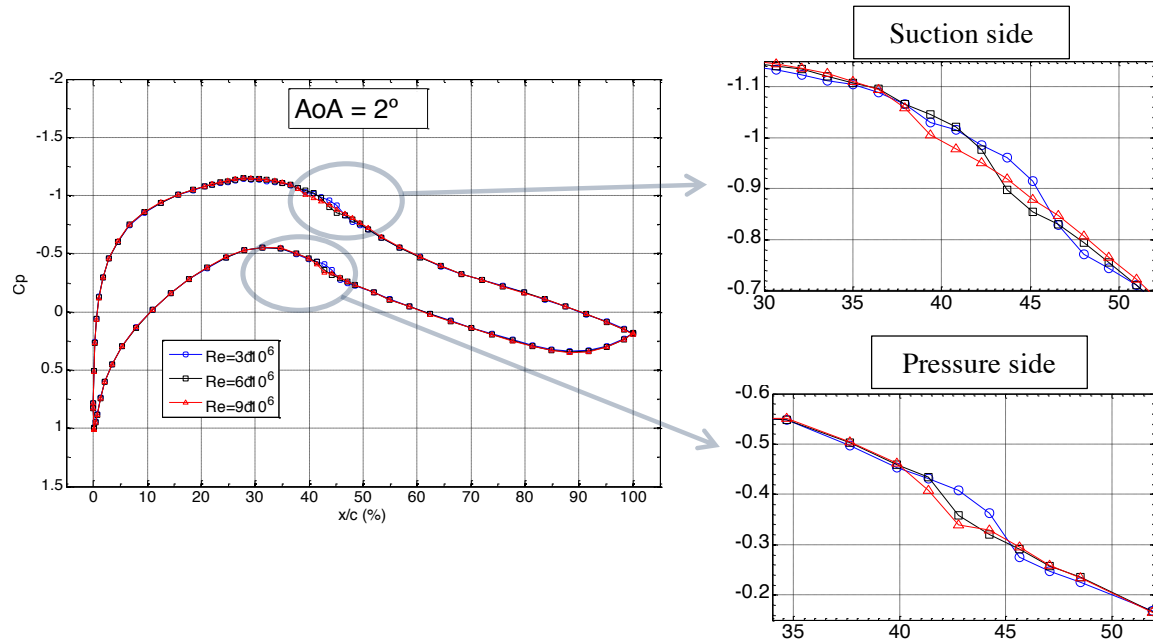


Figure 6. Pressure distribution at $\text{AoA } 2^\circ$ (clean) for 3 Reynolds numbers. Zoom of transition area.

The efficiency (lift to drag ratio: C_l/C_d) against AoA is shown in figure 7 for the different Reynolds numbers. Two main phenomena influence the variation of the maximum efficiency value with Reynolds number. On one side, the move of the drag bucket to lower drag values as the Reynolds number rises implies an increase of the maximum efficiency value. But on the other side, the width reduction of the laminar bucket as the Reynolds number increases, produces a decrease of maximum efficiency values. In the case of this airfoil, the second phenomenon has more impact and the maximum efficiency gets reduced as Reynolds number increases. Out of this angle of attack range of maximum efficiency, the efficiency values are always bigger for higher Reynolds numbers.

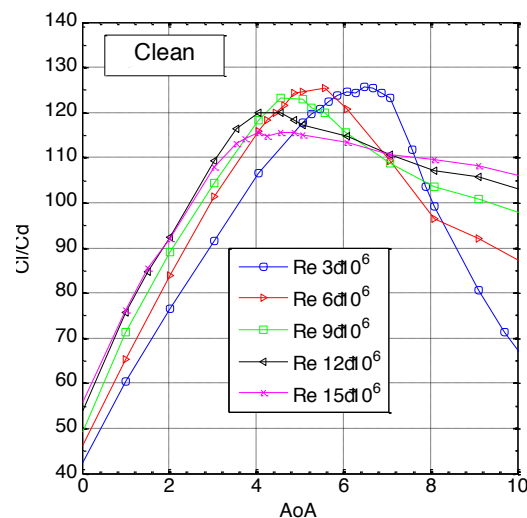


Figure 7. Efficiency variation with Reynolds number for clean condition

Another interesting issue that we can appreciate on figure 7 is how the efficiency curve is sharper for the lower Reynolds numbers and keeps transforming into curves with a top flatter area as the Reynolds number increases. This is an advantage for the higher Reynolds number conditions, since in those cases, the range of AoA with high efficiency is wider and therefore the reduction of efficiency when the AoA moves from the design point is lower.

3.2. Data for the DU00-W-212 airfoil at forced transition conditions

For the tripped cases, not all the angles of attack were measured during the tests, but at least the positive angles of attack for all the Reynolds numbers were tested. The evolution of the lift and drag with Reynolds number for the tripped cases follow a similar trend as for the clean ones, as it can be seen in figure 8. In this case the overlapping of the C_l vs C_d curves does not happen anymore, since the forced transition eliminates the laminar flow over the airfoil and the bucket corners disappear.

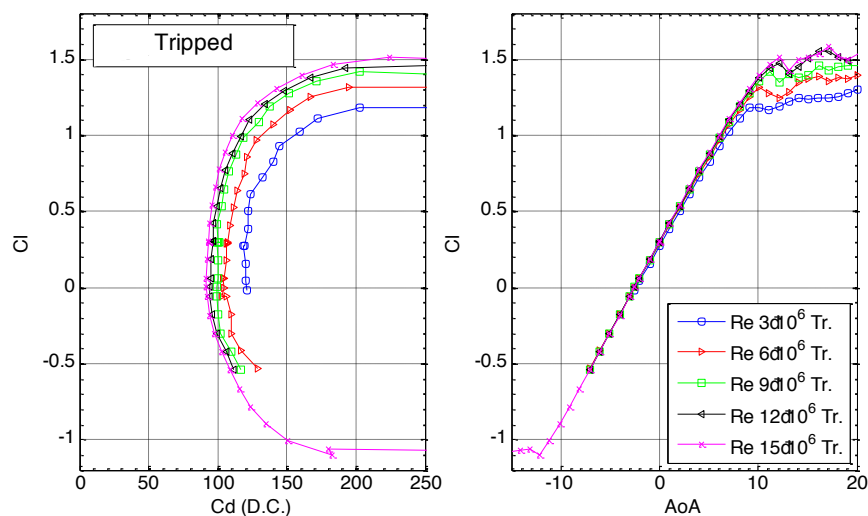


Figure 8. Tripped condition aerodynamic coefficients. Lift vs Drag and Lift vs angle of attack

Since the flow laminarity has been removed, the efficiency curves are now parallel and always increasing with the Reynolds number, as shown in figure 9.

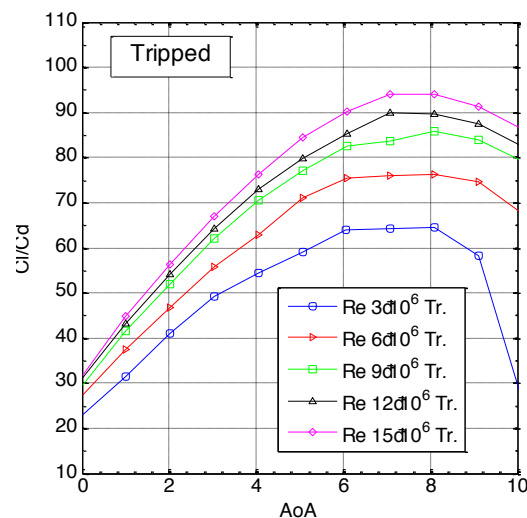


Figure 9. Efficiency variation with Reynolds number for tripped condition

3.3. Comparison of the evolution of aerodynamic parameters with Reynolds number

Figure 10 shows the variations with Reynolds number of some aerodynamic parameters for both clean and tripped cases. The lift slope in the linear region doesn't show variation with Reynolds for the clean case while has some increase for the tripped case. The maximum lift and the minimum drag have very similar trends with Reynolds for clean and tripped conditions.

The maximum lift to drag ratio (efficiency) evolution with Reynolds has opposite behavior for clean and tripped cases as we have explained above. It is always increasing for the tripped condition, but in the clean case is constant at the lower Reynolds number and decreases for the higher ones.

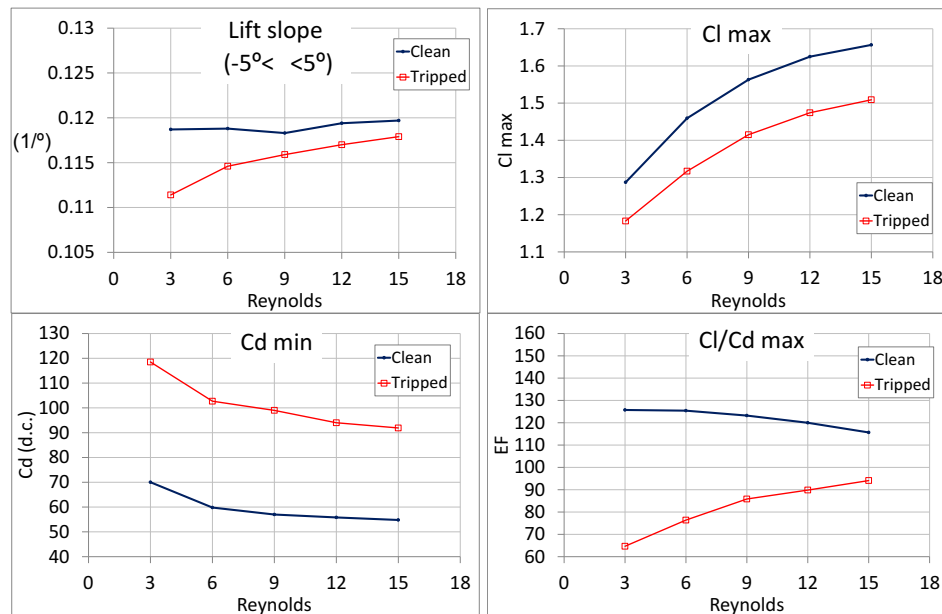


Figure 10. Aerodynamic parameters variation with Reynolds number

4. Conclusions

Reliable experimental data of an airfoil at high Reynolds numbers and low Mach numbers have been measured. This is the first time that a wind turbine airfoil has been measured up to a Reynolds number of 15 million, and it is a good opportunity to analyse the effect of the Reynolds number on its aerodynamic characteristics. The obtained data is of great help on the development and validation of computational codes for the next generation of multi-MW wind turbine designs.

Although the analysis of the data is only applicable to the particular airfoil DU00-W-212, it also gives information about the quantitative variations that airfoil aerodynamic behavior can have at high Reynolds numbers.

The principal aerodynamic parameters evolution has been analysed in the range from 3 to 15 million Reynolds number. The maximum lift coefficient has an increase of 29% in the free transition (clean) case and 28% in the forced transition (tripped) case. The minimum drag coefficient is reduced in a 22% for both clean and tripped condition. The maximum efficiency decreases an 8% for the clean case while increases a 45% for the tripped case.

As it can be seen by the different plots, the increment of Reynolds numbers has benefits for the airfoil aerodynamic behavior in both clean and tripped conditions. The drag gets reduced and the maximum lift increased. Although the maximum efficiency values only increase for the tripped case, the efficiency curve for clean cases has an increase with Reynolds number of the range of AoA at high efficiencies.

References

- [1] Schepers G J et al *Latest results from the EU project AVATAR: Aerodynamic modelling of 10 MW wind turbines* . Science of Making Torque 2016
- [2] Amecke J 1986 *Direct calculation of wall interferences and wall adaptation for two-dimensional flow in wind tunnels with closed walls*. NASA TM-88523
- [3] Allen H J and Vincenti WG 1947 *Wall interference in a two-dimensional wind tunnel, with consideration of the effect of compressibility* NACA Report no. 782
- [4] Abbott H I, et al 1944 *Summary of Airfoil Data* NACA report no.824
- [5] Llorente E, et al 2014 *Wind Tunnel Tests of Wind Turbine Airfoils at High Reynolds Numbers*. Science of Making Torque 2014
- [6] Sommers D M and Tangler J L 2000 *Wind-Tunnel Tests of Two Airfoils for Wind Turbines Operating at High Reynolds Numbers* NREL CP-500-27891
- [7] Loftin K L Jr, Bursnall W J 1948 *Effects of Variations in Reynolds Number Between 3.0×10^6 and 25×10^6 upon the Aerodynamic Characteristics of a number of NACA 6-Series Airfoil Sections* NACA-TN-1773
- [8] Timmer W A 2009 *An overview of NACA 6-digit airfoil series characteristics with reference to airfoils for large wind turbine blades* AIAA 2009-268